# Analysis of VAWT aerodynamics and design using the Actuator Cylinder flow model

**HAa Madsen, US Paulsen, L Vitae**
Department of Wind Energy, Technical University of Denmark, Frederiksborgvej 399, DK-4000, Roskilde

E-mail: hama@dtu.dk

**Abstract.** The actuator cylinder (AC) flow model is defined as the ideal VAWT rotor. Radial directed volume forces are applied on the circular path of the VAWT rotor airfoil and constitute an energy conversion in the flow. The power coefficient for the ideal as well as the real energy conversion is defined. The describing equations for the two-dimensional AC model are presented and a solution method splitting the final solution in a linear and non-linear part is briefly described. A family of loadforms approaching the uniform loading is used to study the ideal energy conversion indicating that the maximum power coefficient for the ideal energy conversion of a VAWT could exceed the Betz limit. The real energy conversion of the 5MW DeepWind rotor is simulated with the AC flow model in combination with the blade element analysis. Aerodynamic design aspects are discussed on this basis revealing that the maximum obtainable power coefficient for a fixed pitch VAWT is constrained by the fundamental cyclic variation of inflow angle and relative velocity leading to a loading that deviates considerably from the uniform loading.

## 1. Introduction

Vertical Axis Wind Turbines (VAWT´s) have in recent years been reconsidered for use in the MW size and not least for offshore, floating concepts where the low centre of gravity of the rotor is one of the advantages. In the DeepWind project [1],[2],[3] a strongly simplified 5MW floating VAWT is being developed. One of the key features is that the water is used as bearing for the rotating floater extending directly from the main shaft, Figure 1.The subject of the paper is an analysis of the fundamental aerodynamic characteristics of the VAWT rotor with focus on the ideal and real energy conversion forming the basis for the actual VAWT rotor design in the DeepWind project.

In the past several flow models for VAWT´s have been developed with different complexity. The multiple stream tube (MST) model by Strickland [4] and the double multiple stream tube (DMST) model by Paravischivoiu [5] have been widely used for aerodynamic analyses. The MST and the DMST models have their origin from the very common blade element momentum (BEM) model used for horizontal axis wind turbines (HAWT´s) and are popular due to their robustness and low computing requirements. In the other end of model complexity is for example the free vortex model by Ferreira [6] which enables computation of flow details around the rotor such as the trailed and shed vortices.

Although widely used, the stream tube models have some build in drawbacks; they are one-dimensional and they are modelling the flow through a plane actuator disc (AD) or a tandem set of AD´s (DMST model) which do not fit to the curved surface of the VAWT turbine. Therefore, the so-

called Actuator Cylinder (AC) model will be used in the present study for modelling the flow through the VAWT rotor and for investigation of the ideal and real energy conversion in this type of rotor.

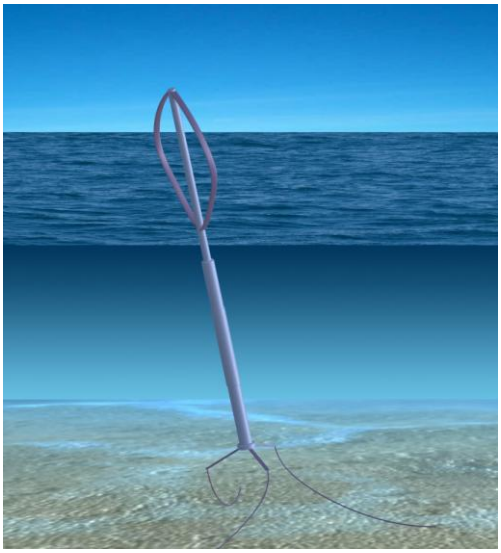

**Figure 1.** The DeepWind floating turbine concept [1],[2],[3].

## 2. The Actuator Cylinder flow model

The AC model was developed from 1979 to 1982 during the PhD study of Madsen [7],[8]. The basic idea behind the development of the model is to extend the well-known AD concept for HAWT´s to a general application of an actuator surface coinciding with the swept area of the actual turbine. For a straight bladed VAWT the swept surface is cylindrical and this is the surface geometry which the model has been developed for in its present form. Further, the model is in a two-dimensional (2D) version in order to limit the complexity of the model and thus e.g. make it suitable for implementation in an aeroelastic code.

Following the AD concept, the reaction of the blade forces in the AC model are applied on the flow as volume or body forces perpendicular and tangential to the rotor plane, respectively, Figure 2. We define the normal and tangential loading $Q_n(\theta)$, $Q_t(\theta)$ as:

$$Q_n(\theta) = B\frac{F_n(\theta)\cos(\varphi) - F_t(\theta)\sin(\varphi)}{2\pi R} \tag{1}$$

$$Q_t(\theta) = -B\frac{F_t(\theta)\cos(\varphi) + F_n(\varphi)\cos(\varphi)}{2\pi R} \tag{2}$$

where $B$ is the number of blades, $R$ rotor radius, $F_n$ is the blade force per unit length perpendicular to the chord, $F_t$ is the blade force per unit blade length parallel to the chord and $\varphi$ is the blade pitch angle as shown in Figure 3.

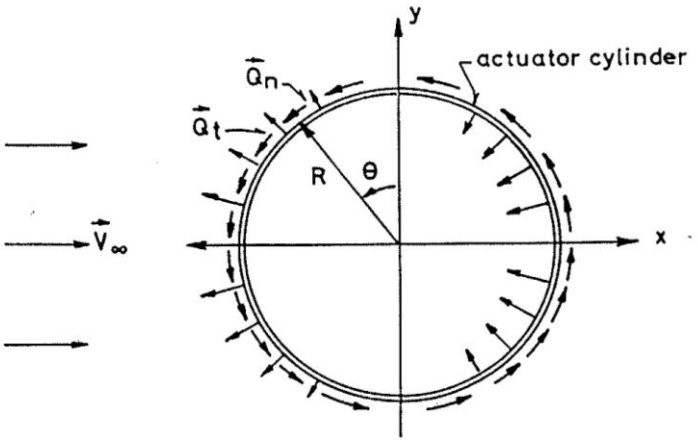


**Figure 2.** The actuator cylinder flow model with radial and tangential loading.

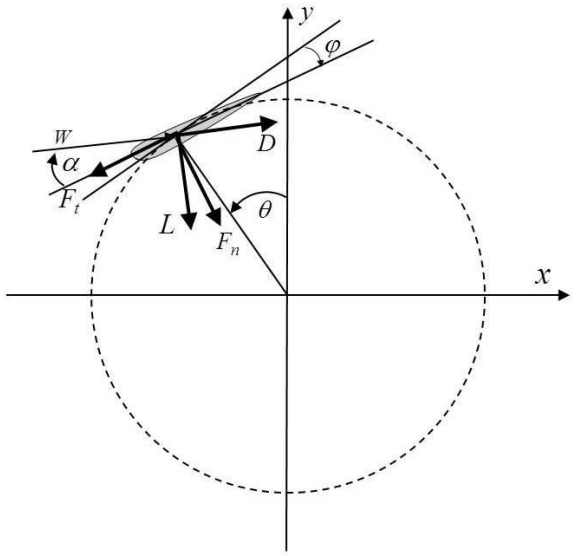


**Figure 3.** The notation in the blade element analysis.

The volume forces $f_n$ and $f_t$ are determined by the equations:

$$Q_n(\theta) = \lim_{\varepsilon \to 0} \int_{R-\varepsilon}^{R+\varepsilon} f_n(\theta) ds \tag{3}$$

$$Q_t(\theta) = \lim_{\varepsilon \to 0} \int_{R-\varepsilon}^{R+\varepsilon} f_t(\theta) ds \tag{4}$$

where $R$ is rotor radius and $\varepsilon$ is a small distance in radial direction. We define the ideal VAWT as a rotor with only radial loading which corresponds to a rotor with zero airfoil drag and with an infinitely high tip speed ratio $\lambda$ defined as:

$$\lambda = \frac{R\Omega}{V_\infty} \tag{5}$$

For the ideal rotor the power conversion $P_i$ can be derived as:

$$P_i = \int_0^{2\pi} v_n(\theta) Q_n(\theta) R \, d\theta \tag{6}$$

where $v_n(\theta)$ is the velocity component perpendicular to the actuator cylinder surface. The ideal power coefficient $C_{Pi}$ is now defined by:

$$C_{pi} = \frac{P_i}{\frac{1}{2}\rho V_\infty^3 2R} = \frac{\int_0^{2\pi} v_n(\theta) Q_n(\theta) d\theta}{\rho V_\infty^3} \tag{7}$$

and the local, ideal power coefficient $C_{pi,l}$ by:

$$C_{pi} = \frac{v_n(\theta) Q_n(\theta)}{\rho V_\infty^3} \tag{8}$$

The real power $P$ is derived as:

$$P = \frac{1}{2\pi} \int_0^{2\pi} B\left( F_t(\theta)\cos(\varphi) + F_n(\theta)\sin(\varphi) \right) R \Omega \, d\theta \tag{9}$$

and the corresponding power coefficient $C_p$ by:

$$C_p = \frac{P}{\frac{1}{2}\rho V_\infty^3 2R} = \frac{\frac{1}{2\pi} \int_0^{2\pi} B\left( F_t(\theta)\cos(\varphi) + F_n(\theta)\sin(\varphi) \right) \Omega \, d\theta}{\rho V_\infty^3} \tag{10}$$

and finally the rotor thrust coefficient $C_T$:

$$C_T = \frac{\int_0^{2\pi} \left( Q_n(\theta)\sin(\theta) + Q_t(\theta)\cos(\theta) \right) R \, d\theta}{\frac{1}{2}\rho V_\infty^2 2R} = \frac{\int_0^{2\pi} \left( Q_n(\theta)\sin(\theta) + Q_t(\theta)\cos(\theta) \right) d\theta}{\rho V_\infty^2} \tag{11}$$

We have now defined a model which enables the analysis of the ideal as well as the real energy conversion in a VAWT rotor. The definition of the ideal energy conversion is the basis for evaluation of the performance of real rotor designs as we now have an upper limit to compare with. Furthermore the ideal rotor provides information on how to improve the design and layout of a real rotor. The ideal energy conversion will be discussed in Section 4 and real rotor designs with particular focus on the 5MW Deepwind rotor will be dealt with a Section 5.

However, before we are able to derive the performance characteristics for the VAWT, the flow field determined by the applied forces on the flow must computed by. One possible solution method is simply to use a standard CFD code and apply the loading given by the body forces in equation 3 and 4. In this case, however, the body forces should be applied over a finite radial distance $\Delta r$ (e.g. equal to 5% of R) in order to obtain a finite intensity of the body forces necessary in the CFD code.
In the present paper we will use the solution method from [7] which is a method where the final solution is split into a linear part being valid for a lightly loaded rotor and a non-linear part necessary to include if it is a heavily loaded rotor. The linear part is very fast to compute numerically and has even been solved analytically for one type of loading on the AC [7].

**3. Describing equations and method of solution**
The describing equations for the two-dimensional flow around an AC have been derived in [7],[8] and will only be briefly described here.
The basic equations are the Euler equations in 2D and the velocity components are written as:

$$v_x = 1 + w_x \quad and \quad v_y = w_y \tag{12}$$

in order to derive the solution to the equations in a linear and a non-linear term. It should be noted that the equations are non-dimensionalized with the basic dimensions $R, V_\infty \; and \; \rho$.
Now the Euler equations take the form:

$$\frac{\partial w_x}{\partial x} + w_x \frac{\partial w_x}{\partial x} + w_y \frac{\partial w_x}{\partial y} = -\frac{\partial p}{\partial x} + f_x \tag{13}$$

$$\frac{\partial w_y}{\partial x} + w_x \frac{\partial w_y}{\partial x} + w_y \frac{\partial w_y}{\partial y} = -\frac{\partial p}{\partial y} + f_y \tag{14}$$

and the equation of continuity:

$$\frac{\partial w_x}{\partial x} + \frac{\partial w_y}{\partial y} = 0 \tag{15}$$

The equations are then rewritten as:

$$\frac{\partial w_x}{\partial x} = -\frac{\partial p}{\partial x} + f_x + g_x \tag{16}$$

$$\frac{\partial w_y}{\partial x} = -\frac{\partial p}{\partial y} + f_y + g_y \tag{17}$$

where $g_x, g_y$ are induced or second order forces defined by:

$$g_x = -\left( w_x \frac{\partial w_x}{\partial x} + w_y \frac{\partial w_x}{\partial y} \right) \tag{18}$$

$$g_y = -\left( w_x \frac{\partial w_y}{\partial x} + w_y \frac{\partial w_y}{\partial y} \right) \tag{19}$$

The following Poisson type equation can then be derived for the pressure:

$$\frac{\partial^2 p}{\partial x^2}+\frac{\partial^2 p}{\partial y^2}=\left(\frac{\partial f_x}{\partial x}+\frac{\partial f_y}{\partial y}\right)+\left(\frac{\partial g_x}{\partial x}+\frac{\partial g_y}{\partial y}\right) \tag{20}$$

Once the pressure field has been found the velocities can be derived by integrating the equations (13) and (14). This means that we can write our final solution as a sum of a linear part and a nonlinear part:

$$w_x = w_x(f)+w_x(g) \quad and \quad w_y = w_y(f)+w_y(g) \tag{21}$$

Due to the limited space in this paper we will just show the linear solution for the normal force loading on the AC:

$$w_x = -\frac{1}{2\pi}\int_0^{2\pi} Q_n(\theta)\frac{-x(x+\sin(\theta))\sin(\theta)+(y-\cos(\theta))\cos(\theta)}{(x+\sin(\theta))^2+(y-\cos(\theta))^2}d\theta - Q_n(\arccos(y))^* + Q_n(-\arccos(y))^{**} \tag{22}$$

$$w_y = -\frac{1}{2\pi}\int_0^{2\pi} Q_n(\theta)\frac{-x(x+\sin(\theta))\cos(\theta)-(y-\cos(\theta))\sin(\theta)}{(x+\sin(\theta))^2+(y-\cos(\theta))^2}d\theta \tag{23}$$

The term marked with $^*$ in Equation (22) shall only be added inside the cylinder whereas in the wake behind the cylinder both the term marked with $^*$ and $^{**}$ shall be added. It can be seen that contrary to the stream tube models, the velocities at one position in the present model are influenced by the loading on the whole blade path. Assuming piecewise constant loading within a certain angle interval, e.g. 10 deg. as used in the present simulations, the integral can be worked out once for all within the same angle interval and constitute a set of influence coefficients between loading and induced velocities which leads to a fast numerical scheme.
As mentioned above more details on the solution procedure can be found in [7],[8].

## 4. Results on the ideal energy conversion

### *4.1. Loadform*

In the study of the ideal energy conversion the loading is not linked to a specific rotor design but instead simply specified without constrains. From the derivation of the Betz limit for the maximum performance of the HAWT type rotor it is known that the uniform loading is the optimal loading and therefore results from runs of a series of loadforms approaching a uniform loading will be shown. The reason for not going directly to the uniform loading is that this loadform introduces very strong flow gradients at the edge of the streamtube encompassing the rotor and as only a numerical solution method is possible this could introduce disturbing numerical uncertainties.
The set of loadforms used can be written on the form:

$$Q_n(\theta) = Q_{n,\max}\frac{\sin(\theta)}{|\sin(\theta)|}\left(1-|\cos(\theta)|^m+\frac{1}{2\pi}\sin\left(2\pi|\cos(\theta)|^m\right)\right) \tag{24}$$

where $Q_{n,\max}$ is a constant and $m$ is an integer parameter which for increasing value will tend to give a more and more uniform loadform as shown in Figure 4a where the number in the loadform legend is the value of m. The specific loadform shown for each $m$ in Figure 4a is the loading expressed by the thrust coefficient $C_T$ that gave the maximum power coefficient, determined from the power coefficient curves in Figure 5. From Figure 5 can be seen that the maximum $C_{pi}$ increases with increasing

$m$ values and that it also occurs at an increasing $C_T$. The $C_{pi}$ curve for the AD with uniform loading and determined from the BEM theory is shown for comparison. It is seen that the $C_{pi}$ curves for the AC model correlate well with this curve for high $m$ values where the corresponding loadform approaches the uniform loading. It appears also from Figure 5 that for $m = 20$ the maximum $C_{pi}$ exceeds the Betz limit at a thrust coefficient of about 0.97. Due to the uncertainties in the numerical simulations this is not a final proof for the maximum $C_{pi}$ for a VAWT can exceed the Betz limit but a strong indication. It should also be emphasized that a major difference to the Betz limit of the AD model is the two stage power conversion in the AC model as the flow passes the volume forces on the front part as well as on the leaward part creating a power conversion along the whole periphery as seen by the local power coefficient as function of azimuth position in Figure 4b. From Figure 4b it is also seen that the major part of the energy conversion with this type of symmetrical loadforms is on the front part of the AC model.

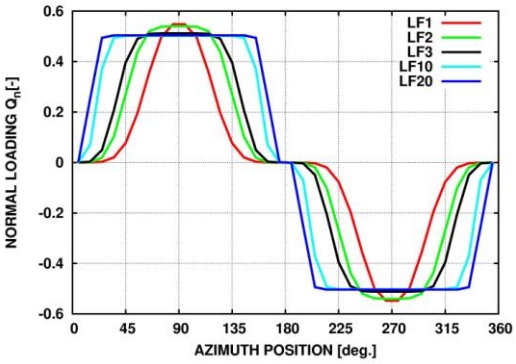


**Figure 4a.** The different loadforms as function of azimuth position at maximum ideal power coefficient.

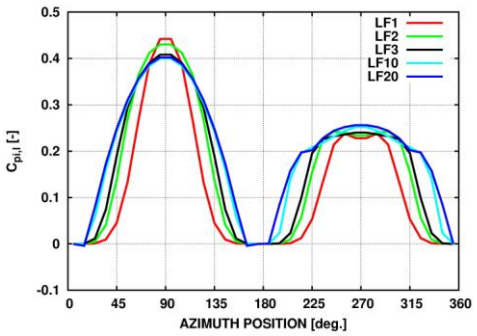


**Figure 4b.** The local power coefficient for the loadforms in Figure 4a.

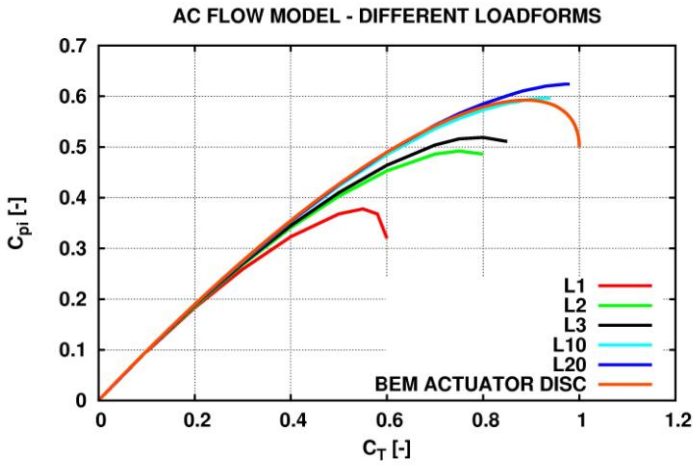


**Figure 5.** The ideal power coefficient for different loadforms on the actuator cylinder in comparison with the ideal power coefficient for a uniform loading on an actuator disc (BEM theory).

*4.2. Asymmetrical loadform*

The unequal distribution of the power conversion, Figure 4b, for the loadforms just presented with the same loading on the upstream and downstream part indicates that it might be more optimal with an asymmetrical loading that gives a more equal power conversion on the two rotor parts. The LF20 loadform was therefore offset with a constant so that the loading on the leeward side of the rotor was

increased and lowered on the windward side as seen in Figure 6a. This caused the local power coefficient to be close to each other on the two parts of the rotor, Figure 6b. However, the integral maximum power coefficient turned out to be exactly the same, $0.633$ for the two loadforms.

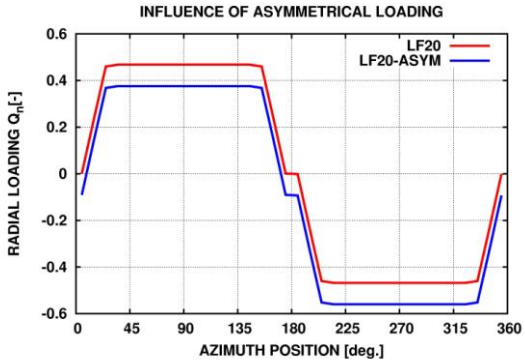


**Figure 6a.** The asymmetrical loading is obtained by subtracting a constant value from the loadform LF20.

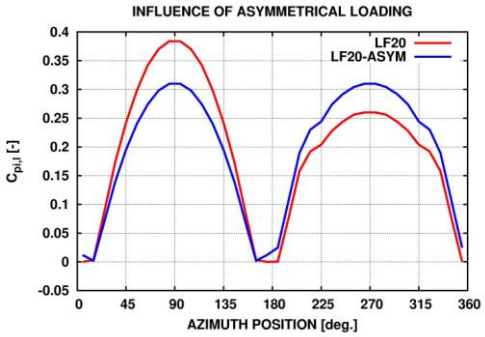


**Figure 6b.** The local power coefficient for the loadforms in Figure 6a.

## 5. The real power conversion and discussion of the 5MW Deepwind design

*5.1. 5MW baseline turbine*

A 5MW Darrieus baseline floating turbine has been developed in the DeepWind project to study the basic aerodynamic performance, the system dynamics and the design of the major component [9]. In the present investigation a simplified, straight bladed version of the baseline rotor will be used for discussion of aerodynamic design aspects using the AC model. The rotor will be modelled assuming fully 2D flow and no blade tip losses. The overall rotor design parameters are:

| | |
|---|---|
| rotor radius $R$: | 63.74m |
| blade chord $c$: | 7.45m |
| airfoil: | NACA0018 |
| number of blades: | 2 |
| solidity: | $\sigma = \frac{Bc}{R} = 0.23$ |
| rated power: | 5000kW |
| rated speed | 5.26rpm |
| swept area: | 10743m$^2$ |
| rotor height $H$: | 84.27m (cylindrical rotor) |

The computed overall rotor characteristics are shown in Figure 7a. The power coefficient $C_p$ reaches its maximum of 0.527 at a tip speed ratio of 3.5 which is a relatively high value and probably due to optimistic airfoil data with a minimum drag coefficient of 0.005. The ideal power coefficient is also shown and at a tip speed ratio of 3.0 the difference between $C_{pi}$ and $C_p$ is only 0.02 which shows that the losses due to airfoil drag are low. The rotor power curve is shown in Figure 7b and has been computed on the assumption of variable speed at optimal tip speed ratio up to 9 m/s and then at a constant speed of 4.5 rpm which is somewhat lower than what was shown above. However, this was necessary to reach a maximum rotor power by stall control for this straight bladed turbine not too much above 5MW.

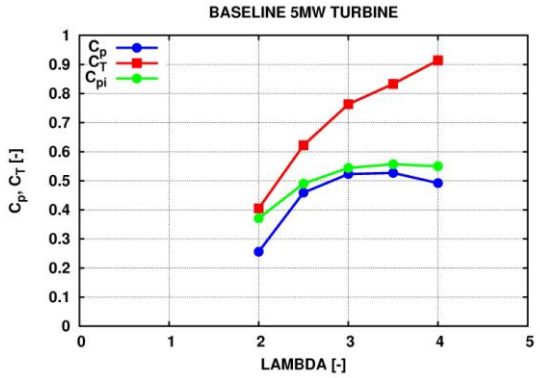


**Figure 7a.** Power and thrust coefficients for the baseline DeepWind rotor

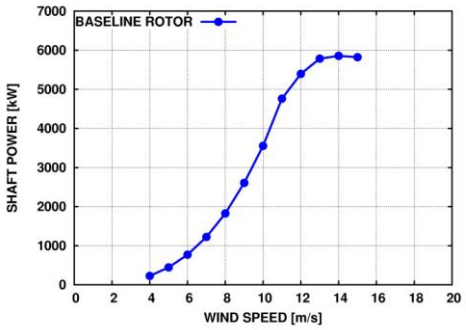


**Figure 7b.** The power curve for the baseline DeepWind rotor.

*5.2. Comparison of 5MW loading with previous ideal loadforms*

The loading on the 5MW turbine at maximum $C_p$ is now compared with the previously investigated loadforms in Section 4 and shown in Figure 8a. It can be seen that in particular on the front side of the rotor the real turbine loading is narrower than e.g. loadform LF20 which led to a maximum $C_{pi}$ above 0.60. The same tendency is seen on the local power coefficient in Figure 8b and we can therefore conclude that a fundamental constraint of a fixed pitch VAWT is that the loading is too narrow and should be more distributed over the rotor periphery. This can be obtained with continuous pitch of the blades which probably mainly is an option for a straight blade turbine. For a Darrieus type turbine the loading could be controlled by trailing edge flaps.

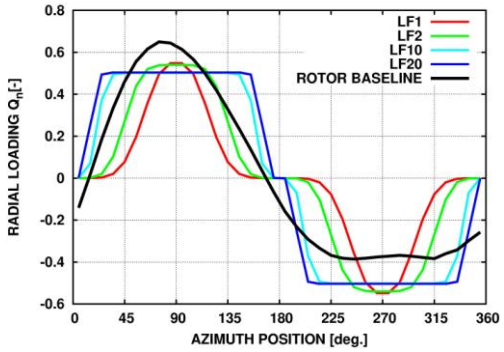


**Figure 8a.** The loading on the baseline rotor at maximum power coefficient in comparison with specified loadforms.

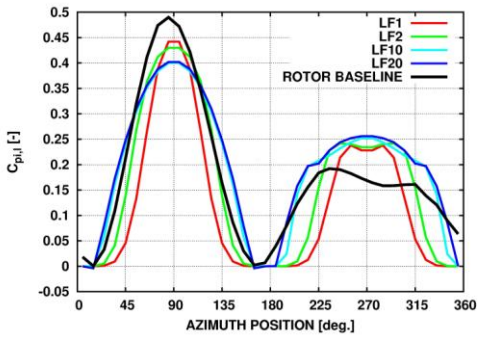


**Figure 8b.** The local power coefficient for the loadforms in Figure 8a.

*5.3. Influence of drag of airfoils and struts*

Influence on rotor performance of an additional constant drag term added at all inflow angles in the airfoil data was investigated because the final structural design could end up with struts to stiffen the blades. Three levels of drag 0.005, 0.010 and 0.015 were simulated and compared with the baseline rotor characteristics, Figure 9a and 9b. It is seen that an increase in drag of 0.001 leads to a reduction of the power coefficient of about 1% but increasing for tip speed ratios above the optimal tip speed ratio.

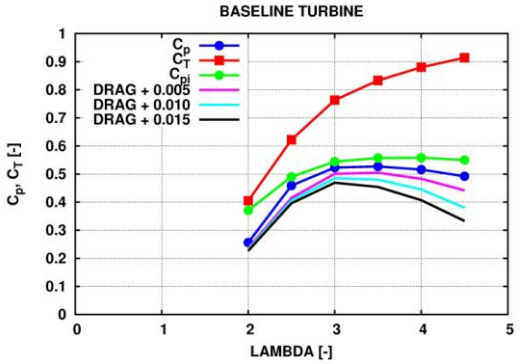


**Figure 9a.** The power coefficient curves for different additional drag values added at all inflow angles in the airfoil data.

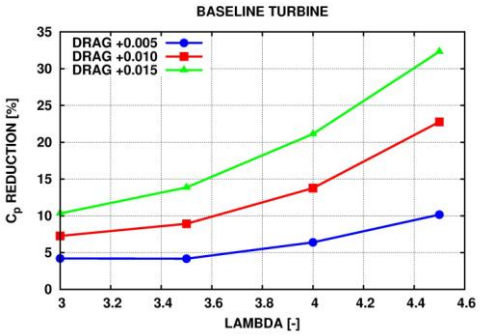


**Figure 9b.** The reduction of the power coefficient for the power coefficient curves in Figure 9a.

## 6. Conclusions

The actuator cylinder flow model has been defined as the ideal VAWT rotor. Radial directed volume forces are applied on the circular path of the VAWT rotor airfoil and constitute an energy conversion in the flow. The maximum power coefficient for the ideal energy conversion seems to exceed the Betz limit and is found for a loadform close to uniform loading. The real energy conversion of the 5MW DeepWind rotor has been simulated with the AC flow model in combination with blade element analysis. It was found that the maximum obtainable power coefficient for a fixed pitch VAWT is constrained by the fundamental cyclic variation of inflow angle and relative velocity leading to a loading that deviates considerably from the uniform loading. A variable pitch of the blades or continous control of lift by flaps could improve the loading. Finally, it was found that an increase in airfoil drag of 0.001 leads to a 1% decrease in power coefficient.

## References

[1] Paulsen U et al. 2011 DeepWind – an innovative wind turbine concept for offshore. Paper presented at EWEA 2011, 14-17 of March, Brussels, Belgium, Organizer European Wind Energy Association

[2] Vita L, Paulsen US, Pedersen TF, Madsen HAa and Rasmussen F 2009 A novel floating offshore wind turbine concept. Proceedings of the European Wind Energy Conference and Exhibition, Marseille (FR), 16-19 Mar, In: EWEC 2009 Proceedings online : EWEC, 2009 (6 p.)

[3] Vita L 2011 Offshore floating vertical axis wind turbines with rotating platform Risø DTU, Roskilde, Denmark, PhD dissertation PhD 80

[4] Strickland JH 1975 The Darrieus turbine: a performance prediction model using multiple streamtubes. Albuquerque: Sandia Laboratory.

[5] Paravischivoiu I 2002 Wind turbine design, with emphasis on Darrieus concept. Polytechnic International Pres.

[6] Ferreira CS 2009 The near wake of the VAWT – 2D and 3D views of the VAWT aerodynamics. PhD thesis TU Delft, Printed by Wöhrmann Print Service, Zutphen,

[7] Madsen H Aa 1982 The actuator cylinder – a flow model for vertical axis turbines. PhD thesis (part 2) Aalborg University Centre

[8] Madsen H Aa 1983 On the ideal and real energy conversion in a straight bladed vertical axis wind turbine PhD thesis (part 3) Aalborg University Centre

[9] Paulsen US, Vita L, Madsen HA, Hattel J, Ritchie E, Leban KM, Berthelsen PA, Carstensen S 2012 1st DeepWind 5 MW baseline design, Proceedings of the DeepSea Conference, 19-20 January 2012, Trondheim, Norway, 2011 Published by Elsevier Ltd.